International Research Journal of Multidisciplinary Scope (IRJMS),2026; 7(1):1389-1407 IRJMS

Original Article | ISSN (O): 2582-631X DOI: 10.47857/irjms.2026.v07i01.08027

Superpixel-Based Image Segmentation with Adaptive Erosion for Waterbody Detection in Flood Prediction

Jyothish VR[1]*, Sajimon Abraham[2], Leo Abraham[3], Sabu Augustine[4]

[1]School of Computer Sciences, Mahatma Gandhi University, Kottayam, India, [2]D School of Management and Business Studies (SMBS), Mahatma Gandhi University, Kottayam, India, [3]Trellix, India, [4]Amal Jyothi College of Engineering, Kottayam, India. *Corresponding Author's Email: jyothishvr1995@gmail.com

Abstract

Severe flood events in India highlight the urgent need for efficient flood management and reliable forecasting systems. One of the biggest obstacles to improving the efficiency of flood monitoring systems is the lack of trustworthy data during flood events. Over the past ten years, computer vision-based methods have become a promising answer for flood monitoring due to recent advancements in information technology. In order to effectively interpret image information and enable meaningful study of flood-affected regions, these approaches mainly rely on robust image segmentation techniques. It is critical for disaster management, particularly in flood forecasting, where precise waterbody detection is essential. However, distinguishing water from visually similar elements such as rooftops, land, and various shades of brown water remains challenging under varying environmental conditions. Traditional methods suffer from misclassification and over-segmentation, affecting prediction accuracy. To address these limitations, we propose a novel superpixel-based segmentation method enhanced with an adaptive erosion technique. Superpixel segmentation effectively groups similar pixels, simplifying image analysis and interpretation, while erosion refines boundaries by removing irrelevant pixel clusters, improving clarity. The final segmentation output is created by applying RGB thresholding to identify water pixels, refining the result using binary erosion, then superimposing the refined mask onto the original colour image. Our method achieves a 1.3% improvement in Jaccard Index, a 3.3% improvement in Recall, a 72.3% enhancement in Boundary F1 Score, and a twofold reduction in computational runtime compared to the SLIC superpixel method, making it a robust tool for flood pre- diction applications.

Keywords: Adaptive Erosion, Computer Vision, Flood Forecasting, Image Segmentation, RGB Thresholding, Superpixel.

Introduction

Floods are becoming a serious problem, causing loss of life, property damage, and health risks. They also harm farmland, reducing crop yields and affecting a country's economy. Early flood warning systems can help reduce the risks and losses caused by flooding (1). To better understand and predict floods, experts from different fields such as hydrology, remote sensing, and meteorology are work together. This teamwork improves flood forecasting, leading to better preparation and response to future floods (2).

The necessity of efficient flood management is shown by recent severe flood incidents in India. Driven by monsoon rainfall that was 42% over average, the 2018 Kerala floods impacted 13 districts, displaced over 1.4 million people, and cost the state's economy more than ₹26,000 crore. Similar to this, Cyclone Michaung caused the December 2023 floods in Tamil Nadu, which recorded up to 93 cm of rain in just two days and seriously damaged residential areas, transport and infrastructure. These occurrences demonstrate the increasing severity of floods and emphasize the necessity of effective floodwater detection and dependable early warning systems.

However, accurately identifying floodwater remains a major challenge, as water bodies often share visual similarities with other surfaces such as rooftops, bare land, and different shades of muddy or sediment- laden water. These similarities become more pronounced under changing environmental conditions, including variations in lighting, cloud cover, and the presence of vegetation (3). Traditional remote sensing techniques may struggle to differentiate floodwater from other elements, especially in urban areas where buildings and roads reflect light in ways that can mimic water surfaces. Although advanced image processing techniques such as superpixel segmentation, spectral analysis and deep learning models have

(Received 04th September 2025; Accepted 13th January 2026; Published 31st January 2026)

improved water detection accuracy in flood mapping, misclassification remains a challenge in complex environments.

To overcome the challenges of waterbody misclassification in flood mapping, this study introduces a novel superpixel-based segmentation approach combined with an adaptive erosion technique. Superpixel segmentation efficiently clusters similar pixels, streamlining image analysis and interpretation, while adaptive erosion dynamically fine-tunes boundary refinement by eliminating irrelevant pixel clusters based on local im- age properties. Unlike traditional erosion, which applies a fixed kernel uniformly, adaptive erosion adjusts its intensity based on pixel connectivity and local features, effectively preserving essential structures while removing noise. This ensures that waterbodies are more accurately distinguished from visually similar regions such as rooftops, bare land, turbid water, wet soil, shadows, and vegetation. By preventing over-segmentation, adaptive erosion improves the coherence of superpixel clusters, leading to a more precise representation of water regions (4). Furthermore, this method reduces false positives and computational overhead, enhancing both seg- mentation accuracy and efficiency, making it particularly suitable for real-time flood prediction applications. The proposed research makes several significant contributions:

Enhanced Segmentation Accuracy

Adaptive erosion improves boundary refinement, leading to higher Jaccard Index, recall, and Boundary F1 Score, ensuring precise waterbody detection.

Reduction of Over-Segmentation

By refining superpixel clusters and eliminating irrelevant pixel groups, adaptive erosion prevents over segmentation and enhances segmentation clarity.

Improved Computational Efficiency

Adaptive erosion significantly reduces processing time, making it approximately twice as fast as SLIC-based segmentation, which is crucial for real-time flood prediction applications.

Adaptation to Environmental Variability

Unlike traditional methods, adaptive erosion adjusts its intensity based on pixel connectivity, effectively distinguishing waterbodies from visually similar regions such as wet soil and shadows. Accurate detection and segmentation of floodwater are critical for effective disaster management and mitigation. Traditional remote sensing techniques, such as multispectral and hyperspectral analyses, have been widely employed to map water bodies using satellite imagery (4). However, these conventional methods often face significant challenges in complex urban and semi-urban environments, where surfaces like rooftops, roads, and bare land exhibit spectral characteristics similar to floodwater, leading to frequent misclassifications.

To address these limitations, several deep learning approaches have been explored for flood detection. Table 1 discusses significant studies were conducted in the literature. For instance, a study applied a modified U-Net convolutional neural network (CNN) to satellite images, demonstrating highly effective performance in accurately segmenting flood-affected regions. Similarly, an optimized deep learning model incorporating a hybrid metaheuristic strategy, combining Harris Hawks Optimization (HHO) and Shuffled Shepherd Optimization (SSO), exhibited improved flood prediction capabilities by enhancing feature selection and model robustness (5). Despite these advancements, deep learning models often require extensive labelled datasets, demand significant computational resources, and may face challenges related to the interpretability of their decision-making processes.

Superpixel-based segmentation has emerged as a promising alternative for flood detection. Superpixels group pixels with similar properties into compact clusters, thereby reducing noise and enhancing object boundary representation (6). Among various approaches, the Simple Linear Iterative Clustering (SLIC) algorithm has gained popularity due to its computational efficiency and simplicity (7). SLIC leverages both color similarity and spatial proximity, using a 5D feature space (color and pixel coordinates) for superpixel generation. However, in heterogeneous urban flood scenes, SLIC frequently suffers from over-segmentation, leading to fragmented waterbody regions and increased false positives (8).

While SLIC effectively segments homogeneous regions, it often suffers from over-segmentation in heterogeneous environments like urban flood scenes, leading to fragmented waterbody regions

and increased false positives (8, 9). To overcome this limitation, several enhanced variants of SLIC have been proposed. For instance, an edge-based SLIC (ESLIC) algorithm was developed to improve boundary adherence and preserve weak edges in high-resolution remote sensing images, thereby enhancing segmentation accuracy in flood-prone areas.

Moreover, watershed-based segmentation techniques have also been integrated with superpixel approaches to mitigate over-segmentation issues (10). An enhanced watershed algorithm combining pre-processing and post-processing procedures has proven effective in accurately delineating cultivated land and waterbody boundaries from high-resolution images (11). However, traditional erosion techniques applied for boundary refinement often utilize a fixed structuring element, which may cause the loss of critical waterbody details in noisy or visually complex regions. Recent advancements have introduced adaptive erosion and segmentation strategies that dynamically adjust parameters based on local image properties (12). These adaptive methods refine segmentation boundaries by considering pixel connectivity and contextual features, preserving essential structures while effectively eliminating noise. Despite these developments, challenges remain in accurately distinguishing floodwater from visually similar surfaces under varying environmental conditions, such as lighting variations, cloud shadows, and vegetation presence.

From the literature review, it is observed that most of the existing flood detection techniques rely on machine learning and deep learning models, which require a large amount of labeled data and time-consuming training processes. Additionally, these methods often face difficulties in accurately capturing the boundaries of flooded regions. To address these challenges, this study proposes a superpixel-based image segmentation approach with adaptive erosion for effective waterbody detection in flood-affected regions. The proposed method performs pixel-level analysis, enabling better representation and clear identification of water regions without the need for any training or large labeled datasets.

Table 1: Existing Methods for Waterbody Segmentation in Flood Detection

Technique	Strengths	Limitations	Research Gap	References
Traditional Remote Sensing	Large area coverage, standard approach	Misclassification in urban regions due to spectral similarity with non-water surfaces	Needs robust methods for heterogeneous environments	(4)
Deep Learning Models	High accuracy (e.g., IoU up to 67.35%)	Requires large annotated datasets, computationally expensive, less interpretable	Efficient & explainable models for flood detection	(13)
Superpixel Segmentation	Preserves object boundaries, reduces noise	Over-segmentation in heterogeneous regions	Adaptive parameter tuning for complex environments	(5)
Enhanced SLIC Variants	Better edge adherence, improved boundary detection	Sensitive to noise, fixed parameters may miss fine details	Dynamic segmentation for diverse flood scenarios	(14)
Enhanced SLIC Variants	Better edge adherence, improved boundary detection	Sensitive to noise, fixed parameters may miss fine details	Dynamic segmentation for diverse flood scenarios	(15)
Hybrid Segmentation Techniques	High accuracy (e.g., Dice score up to 98.68%)	May be dependent on image characteristics such as lighting conditions	Robust methods adaptable to varying image conditions	(16)

Methodology

Over-Segmentation Challenges in Waterbody Detection

Pixel-level image segmentation remains a highly challenging task due to the complex distribution and orientation of pixels in an RGB image. The intensity values of pixels are not unique to specific surface types, which often leads to ambiguity in distinguishing between classes. For example, water regions, rooftops, and land surfaces may share similar pixel intensity values, making direct classification at the pixel level prone to errors (17). This issue is particularly critical in flood detection, where accurate separation of inundated areas from non-flooded regions is essential. Superpixel-based segmentation provides an effective alternative by grouping pixels into perceptually meaningful clusters based on homogeneity criteria. Unlike raw pixel-level approaches,

superpixels aggregate local information and preserve object boundaries, resulting in a more structured and interpretable representation of the image (18). This facilitates improved discrimination between visually similar classes and reduces the noise associated with pixel-wise analysis.

One of the primary challenges of the proposed water area segmentation technique is over-segmentation, which arises due to the similarity in pixel values between water and other regions, such as the sky (19). The segmentation algorithm is entirely pixel-focused, and its reliance on predefined RGB value ranges often results in misclassification. Specifically, the sky region exhibits RGB values of [255, 255, 255], which closely resemble the accumulated pixel ranges in the proposed method is represented in Figure 1. This similarity leads to incorrect segmentation, affecting not only the sky area but also elements such as rooftops and land regions (20). During segmentation, pixels that satisfy the predefined criteria are classified as water regions and typically visualized in white. Although this facilitates easier identification, it also increases the risk of false positives, particularly when non-water surfaces exhibit spectral similarity or textural patterns comparable to flooded areas. Such spectral confusion often results in misclassification, reducing the overall accuracy of waterbody delineation.

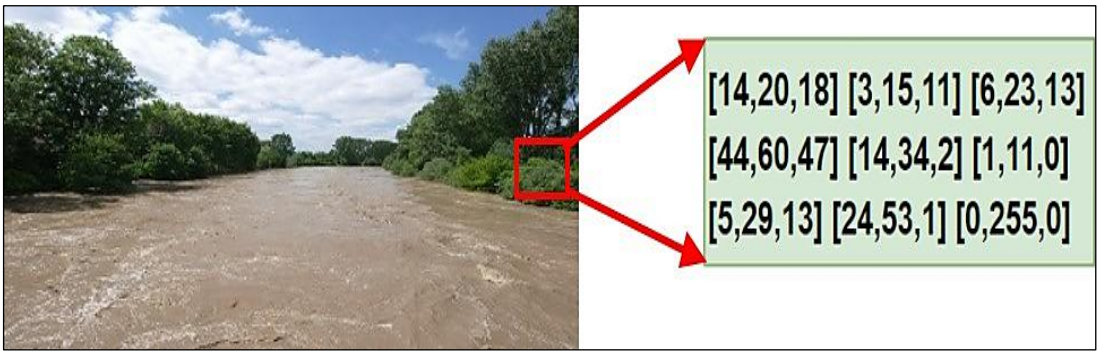

Figure 1: Image with Different Pixel Value Orientation

These inaccuracies impact the overall reliability of the method, making it necessary to refine the pixel classification strategy to minimize over-segmentation and improve the distinction between water bodies and non-water regions in aerial images. Figure 2 illustrates this issue, showing an input image, an expected segmentation mask, and an over-segmented output. The over-segmented regions arise due to pixel intensity similarities between water and other elements in the scene. Figure 2 (A) is the input, showing a body of brown, muddy water surrounded by trees and a bright sky with clouds. Figure 2 (B) shows the ideal segmentation mask, where the water is perfectly isolated in white against a black background. However, the output of the segmentation algorithm, shown in Figure 2 (C), reveals a critical failure: the algorithm has misclassified a large portion of the bright sky and clouds as water. This happens because the pixel intensity values of the bright, foamy parts of the brown water are very similar to those of the clouds. A simple, color-based segmentation method fails to distinguish between these visually similar but contextually different regions. This misclassification leads to an over-segmented output, which would result in a highly inaccurate estimation of the flooded area, making the method unreliable for flood forecasting.

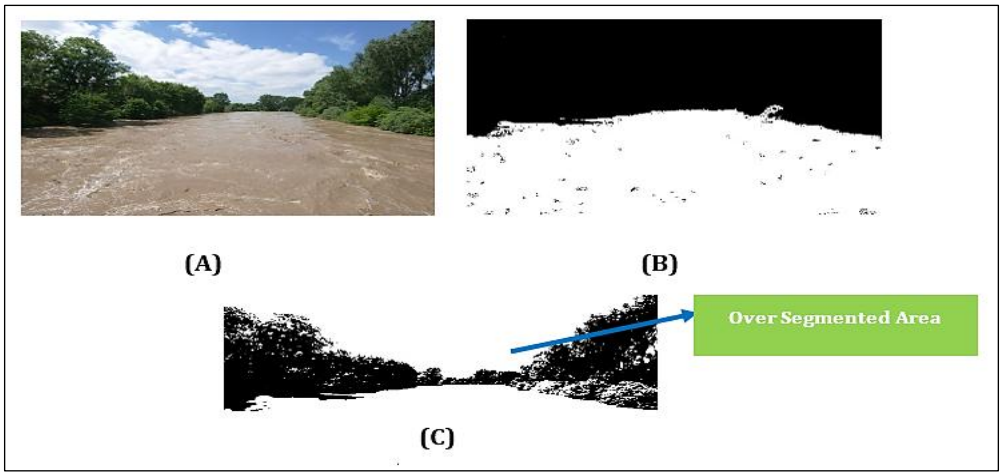

Figure 2: (A) Input Images (B) Expected Segmentation Mask (C) Segmentation Mask with Over Segmented Output

Proposed Adaptive Erosion-Based Segmentation

Adaptive erosion refines the segmentation process by dynamically adjusting the erosion kernel based on local image properties. Unlike traditional fixed-kernel erosion, this method adapts to pixel intensity variations and texture differences, effectively distinguishing water regions from visually similar non-water areas. The adaptive erosion approach reduces noise and false positives while preserving meaningful water structures.

In image segmentation, erosion is a morphological technique that reduces noise and sharpens object boundaries. Erosion creates smoother, more compact areas by eliminating tiny imperfections and weak connections along object edges by the iterative application of a structuring element. Because it helps remove extraneous details while maintaining the essential structure of significant objects like water bodies, this technique is especially useful when precise boundary delineation is needed (21, 22).

In morphological image processing, erosion is formally defined using set theory. Let A denote the input binary image and B the structuring element. The erosion of A by B is given in Equation [1].

$$A \ominus B = \{z \mid (B)_z \subseteq A\} \qquad [1]$$

Where (B)z denotes the translation of B by vector z over the image domain.

The input image and the erosion-related structural element are shown in Figure 3. Unlike fixed-kernel erosion, the suggested adaptive erosion approach dynamically modifies the kernel size based on local picture features. This adaptive selection is ideal for complex flood images because it effectively suppresses heterogeneous noise while maintaining waterbody features.

Although a number of adaptive morphological techniques have been investigated for picture segmentation, including adaptive dilation, opening-closing processes, and multi-scale morphology, these approaches mostly concentrate on region expansion or necessitate careful scale selection, which frequently increases computational complexity. Adaptive erosion, on the other hand, deliberately shrinks ambiguous regions based on local image properties in order to directly target border refinement and noise suppression. Because of this, it is especially useful for floodwater segmentation, where the main difficulty is eliminating spectrally similar non-water areas (such the sky and bright surfaces) while maintaining actual water boundaries.

Different kernel sizes such as 3 × 3, 5 × 5, and 7 × 7 were experimented to study their impact on segmentation performance. The 3 × 3 kernel performed fine-grained erosion, preserving edges and small waterbody regions effectively while removing minor noise. The 5 × 5 kernel offered moderate erosion, suitable for removing larger noise but sometimes impacting smaller waterbody shapes. In contrast, the 7 × 7 kernel caused aggressive erosion, useful for eliminating large noise but often leading to the loss of essential narrow water regions.

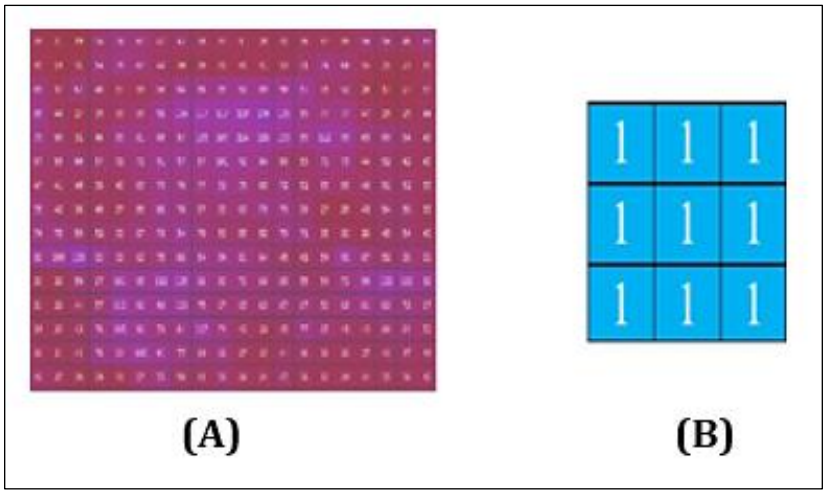

Figure 3: (A) Input Image (B) 3x3 Structuring Element (Kernel)

Adaptive Kernel Selection Strategy

The adaptive erosion strategy is explicitly defined as an image-statistics-based approach, rather than a purely heuristic or manually tuned method. Kernel size selection is guided by quantitative measurements extracted from local image regions.

Mathematical Formalization of the Adaptive Kernel Selection Strategy

Let I denote the input grayscale image and Ω represent a local Superpixel region. For each region, three statistical descriptors are computed,

Local Intensity Variance

Equation [2] represents the Local intensity variance

$$\sigma_{\Omega}^{2} = {}_{N}^{1}\sum_{i\in\Omega}(I_i - \mu\Omega\ )^2 \qquad [2]$$

where μΩ is the mean intensity and N is the number of pixels in the region.

Noise Indicator

Noise level is approximated using local variance, where higher variance indicates stronger noise presence.

Texture Complexity

Texture strength is implicitly captured by intensity variance, with higher values corresponding to more heterogeneous regions.

Kernel Selection Rule

Based on the computed variance $\sigma\Omega^2$, the structuring element size K is selected as equation [3],

$$\boldsymbol{K} = \begin{cases} \boldsymbol{3x3}, & \boldsymbol{if}\ \sigma_{\Omega}^{2} < T_1 \\ \boldsymbol{5x5}, & \boldsymbol{if}\ \sigma_{\Omega}^{2} \leq T_2 \\ \boldsymbol{7x7}, & \boldsymbol{if}\ \sigma_{\Omega}^{2} > T_2 \end{cases} \qquad [3]$$

where T_1 and T_2 are empirically determined thresholds derived from training data statistics.

The experimental analysis validates that these statistically guided kernel choices yield optimal segmentation performance, with the 3×3 kernel achieving the highest average Dice score under low-noise conditions.

Figure 4 represents the change after erosion applied on the image. In this context, the key distinction is that areas other than the water become darker. As a result, the potential for excessive segmentation (breaking down the image into too many small segments) is reduced. Erosion refines images by reducing the influence of random pixels or noise. This noise reduction enhances the accuracy of identifying the image's significant elements, as it removes distractions and isolates the key features.

Figure 4: (A) Input Image for Segmentation (B) Eroded Image

In the context of water area detection, segmentation techniques are employed to identify the regions of interest, which in this case are the water areas. It is apparent that water areas are distributed across various parts of the images, often interspersed with less significant features. In order to emphasize the water areas and minimize the influence of other features, erosion is employed as a pre-processing technique. By applying erosion, the surrounding areas are gradually reduced, while the water areas remain relatively unchanged (23, 24). This process enhances the accuracy of superpixel generation and subsequently improves the segmentation outcomes. Figure 5 depicts improvement before and after the application of erosion technique. By applying adaptive erosion, the surrounding areas are gradually reduced adaptively based on contextual features, ensuring water areas remain relatively unchanged while minimizing over segmentation. Excessive fragmentation is seen in Figure 5 (A), which shows superpixel segmentation prior to erosion. Over segmented superpixels are visible in the corresponding magnified image. On the other hand, Figure 5 (B) shows the superpixel segmentation outcome following the application of adaptive erosion, exhibiting enhanced region consistency. By displaying accurately segmented superpixels with clearly defined borders, the magnified view and further validates the efficacy of the suggested method. This method enhances the accuracy of superpixel generation, leading to more precise segmentation compared to normal superpixel methods.

Superpixel Refinement Using RGB Threshold

In this proposed work, an empirical thresholding technique based on data is employed to determine the RGB threshold ranges needed for superpixel refining. The thresholds are determined by examining several flood-affected photos that show various muddy-water appearances under different lighting and environmental conditions, as opposed to depending on arbitrary or image-specific intuition.

Four RGB variants Narrow, Medium, Proposed, and Wide—were defined in order to assess the impact of colour thresholds on floodwater segmentation. While Medium (R: 80–180, G: 70–160, B: 40–140) permits moderate lighting and sediment changes, Narrow (R: 90–170, G: 80–150, B: 50–120) targets darker brown water, minimizing false positives but running the risk of under-segmentation. The proposed threshold (R: 70–200, G: 71–188, B: 30–180) balances recall and precision while capturing a variety of muddy water appearances. Although it can tolerate high brightness and turbidity, wide (R: 60–220, G: 60–200, B: 20–200) may over segment non-water areas. This process makes it possible to systematically assess segmentation robustness in a variety of flood scenarios.

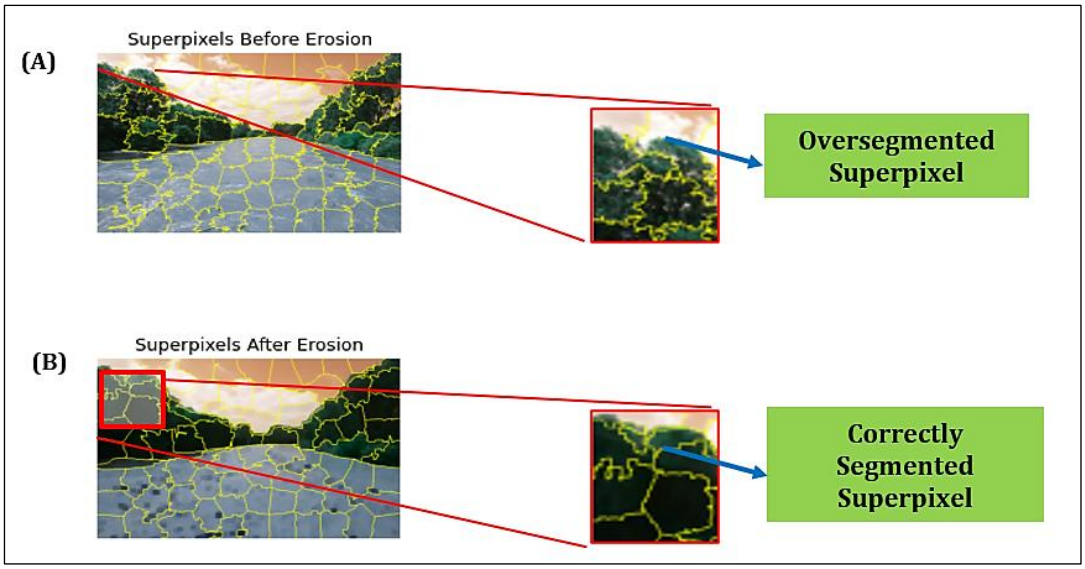

Figure 5: Comparison of Normal Superpixel Segmentation and Adaptive Erosion-Enhanced Superpixel Segmentation: (A) Superpixel Segmentation before Erosion and Enlarged View Highlighting Over segmented Superpixels, (B) Superpixel Segmentation after Applying Adaptive Erosion, and Enlarged View Showing Correctly Segmented Superpixels

Table 2 presents the analysis of randomly selected image samples evaluated using different threshold variants. Based on the segmentation accuracy, the pixel value ranges yielding the highest performance were identified and selected as the proposed RGB threshold values. The flood images dataset was employed to pick the image samples used in this analysis, which ranged from 1.jpg to 10.jpg, to reflect a variety of statistical and visual aspects of floodwater scenarios. RGB-based floodwater segmentation is frequently impacted by fluctuations in illumination, silt concentration, turbidity, backdrop complexity, and local variance, all of which are captured in these images. The chosen images serve as typical test cases for assessing the behaviour of various RGB threshold variants in diverse real-world conditions rather than as isolated visual examples. This method of selection guarantees that the recommended threshold ranges are not skewed towards a particular image or lighting scenario and are instead based on data-driven observations.

Table 2. Dice Similarity Coefficient (DSC) Comparison for Different RGB Threshold Variants

Image Sample	Kernel Size	Local Variance	Threshold Type	Dice Score
1.jpg	5	0.019514	Narrow	0.4866
1.jpg	5	0.019514	Medium	0.8325
1.jpg	5	0.019514	**Proposed**	**0.9530**
1.jpg	5	0.019514	Wide	0.9530
3.jpg	7	0.074995	Narrow	0.8342
3.jpg	7	0.074995	Medium	0.8955
3.jpg	7	0.074995	**Proposed**	**0.9004**
3.jpg	7	0.074995	Wide	0.8810
9.jpg	7	0.026758	Narrow	0.6965
9.jpg	7	0.026758	Medium	0.7932
9.jpg	7	0.026758	**Proposed**	**0.8998**
9.jpg	7	0.026758	Wide	0.9187

Proposed Algorithm

Algorithm 1 explains the water area detection with erosion as preprocessing. It works by starting with input image and creating an empty image (R) that is the same size as input image. It uses a 3x3 square- shaped" kernel" and has a set number of iterations (in this case, 6). For each pixel in input image, the kernel's center is placed on that pixel. The algorithm checks if all the white pixels in the kernel overlap with white pixels in A. If they do, the corresponding pixel in R is set to white. Otherwise,

it's left as is. After processing all the pixels in A, the resulting image R is saved. After generating the output image, the image is processed to create superpixels. The algorithm calculates the average color value (RGB) for each superpixel. If the average RGB values meet specific thresholds, the pixel intensities in the red channel (R) are changed to white (RGB: 255, 255, 255). For superpixels that do not meet the thresholds, the original pixel intensities are kept. This step refines the segmentation by modifying pixel values based on their average color within the superpixels.

The proposed method first identifies potential water pixels in the color image using RGB thresholding. Binary erosion is used to remove small noisy areas and refine borders once this RGB map has been converted to a binary image. Finally, the eroded and corrected binary map is superimposed back onto the original color image to complete the transition from grayscale/binary processing to a visually acceptable color segmentation output.

Algorithm 1 Superpixel-Based Image Segmentation with Adaptive Erosion for Waterbody Detection (with Adaptive Kernel Size Selection)

Input: Input Image A
Output: Refined Segmented Output Image R
1 Read the input image A
2 Initialize an empty output image R of the same size as A
3 Select Structuring Element S (Kernel Size) based on image characteristics:
Fine noise removal → 3 × 3 Kernel Moderate noise removal → 5 × 5 Kernel Large noise removal → 7 × 7 Kernel
4 **Set** the number of erosion iterations N = 6
5 Adaptive Erosion Process:
for each pixel (x, y) in image A **do**
6 **if** R(x, y) < 200, G(x, y) < 200, and B(x, y) < 200 **then**
7 Place the center of selected S at (x, y) if All corresponding pixels under S are white then
8 **Set** pixel (x, y) in R to white (255, 255, 255)
9 Repeat erosion process for N iterations
10 Superpixel Segmentation:
Apply SLIC superpixel segmentation on image R
11 Generate superpixels S1, S2, S3, . . . , Sn
12 **Compute** the average RGB values for each superpixel Si
13 **Adaptive Superpixel Refinement:** for each superpixel Si do
14 **if** 70 ≤ mean(R) < 200, 71 ≤ mean(G) < 188, and 30 ≤ mean(B) < 180 **then**
15 **Set** all pixels in Si to white (255, 255, 255)
16 **else**
17 Retain original pixel values
18 Output the final refined segmented image R

Results and Discussion

To evaluate the effectiveness of the proposed water area segmentation techniques, a series of experiments were conducted using randomly selected flood-affected images from Kerala. The proposed methodology utilizes four key components for accurate waterbody detection: the original input image, corresponding ground truth image, superpixel generated image, and the final segmentation mask. This framework helps in effectively distinguishing water regions from shadows and other background elements present in the images.

Performance Evaluation Metrics

Dice similarity coefficient

To assess the accuracy of image segmentation in more depth, the Dice similarity coefficient (DSC) is employed. This coefficient quantifies the extent to which the segmented image aligns with the original (ground truth) image in terms of spatial overlap. Equation [4] is employed to determine the precision of image segmentation.

$$D(A,B) = \frac{2|A \cap B|}{|A| + |B|} \quad [4]$$

Jaccard Index (Intersection over Union (IoU)

The Jaccard Index measures the similarity between the predicted segmentation and the ground truth. It is defined as the ratio of the intersection over the union of the predicted (A) and actual (B) segments. Equation [5] mathematically represents Jaccard Index as:

$$J(A,B) = \frac{|A \cap B|}{|A \cup B|} \quad [5]$$

A higher Jaccard Index value indicates better segmentation overlap between the predicted output and the ground truth.

Precision

Precision represents the proportion of correctly predicted positive pixels among all pixels predicted as positive. Equation [6] shows the precision calculation.

$$\text{Precision} = \frac{TP}{TP + FP} \quad [6]$$

High precision indicates that the model produces fewer false positives and is effective at avoiding over-segmentation.

Recall

Recall measures the ability of the model to correctly identify all relevant positive pixels. A high recall value indicates the model can capture most of the actual target regions with minimal misses. Equation [7] represents the recall.

$$Recall = \frac{TP}{TP + FN} \quad [7]$$

Boundary F1 Score (BF Score)

The Boundary F1 Score evaluates the accuracy of the predicted object boundaries. It is the harmonic mean of boundary precision (Pb) and boundary recall (Rb). This metric is especially useful for image segmentation tasks where edge accuracy is important.

Runtime

Runtime reflects the computational efficiency of the algorithm and is measured in seconds. Lower runtime values indicate better performance and make the method more suitable for real-time or large-scale applications.

Input Image Quality Analysis

The proposed method is implemented on ten sample images, which were collected from various sources rather than from a single standardized dataset. Instead of using high-quality images, moderately clear images were deliberately chosen to reflect realistic and challenging conditions commonly encountered in flood situations. The method operates at the pixel level, analyzing features such as intensity values, color composition, resolution, and edge quality. This paper focuses on segmenting waterbodies from images with relatively low resolution, demonstrating the model's effectiveness in resource-constrained scenarios. Instead of giving priority to visual quality, the ten input images (1.jpg–10.jpg) were chosen to capture representative variability in flood-affected imagery. The photos represent genuine situations found in flood monitoring scenarios and range in resolution, edge complexity, and visual clarity. By avoiding bias towards ideal images, this choice makes it possible to test the suggested segmentation technique in real-world scenarios that are difficult. Table 3 presents the resolution, edge complexity, and visual quality of the selected input images.

Table 3. Input Image Quality Analysis Based on Resolution, Edge Complexity, and Visual Quality

Image Sample	Resolution (W×H)	Edge Complexity	Visual Quality [1–5]
1.jpg	395×650	3.04	1
2.jpg	512×770	3.57	3
3.jpg	512×683	3.42	3
4.jpg	512×683	5.65	3
5.jpg	512×768	2.67	2
6.jpg	512×764	2.58	2
7.jpg	384×512	5.05	3

8.jpg	384×512	6.66	3
9.jpg	384×512	1.99	2
10.jpg	384×512	3.16	2

To quantitatively evaluate the quality of these inputs, a visual quality metric was employed. This metric ranges from 1 to 5, where 1 denotes poor visual clarity and 5 indicates excellent image quality. Among the ten images, half belong to the low-resolution category, while the other half are considered high-resolution. In real-time flood monitoring scenarios, it is common to encounter noisy and low-resolution imagery due to limitations in acquisition devices or transmission conditions. The proposed algorithm not only performs segmentation but also successfully extracts meaningful pixel-level features from such images, highlighting its robustness.

The diversity in edge complexity and visual quality across the dataset ensures a thorough evaluation of the model's generalization capability. As shown in Table 3, image resolutions range from 384×512 to 512×770, representing a balanced mix of low- and high-resolution cases. Edge complexity, computed using gradient-based analysis, varies significantly—from 1.99 in smoother regions to 6.66 in highly textured or cluttered areas providing an ideal test bed for assessing segmentation accuracy under varying visual conditions.

Performance Enhancement via Adaptive Erosion Strategy

Metric-Based Validation of Segmentation Accuracy and Boundary Delineation

To assess the effectiveness of the proposed Adaptive Erosion method in Table 4 compared to the original SLIC output, we conducted a statistical evaluation using three key segmentation metrics: Over-Segmentation Rate (OSR), Hausdorff Distance, and Boundary F1 Score. The mean and standard deviation were computed for each metric, and the percentage change was calculated to highlight relative performance improvements. The Over-Segmentation Rate (OSR) of Adaptive Erosion (0.7574 ± 0.1462) is nearly identical to that of the SLIC original (0.7550 ± 0.1494), with only a slight increase of 0.32%. This negligible variation indicates that Adaptive Erosion preserves the segmentation balance without introducing additional over-segmentation. In contrast, the Hausdorff Distance—where lower values are desirable—shows a significant improvement with Adaptive Erosion, reducing from 325.83 ± 131.45 (SLIC) to 216.37 ± 94.01, marking a 33.6% decrease. This substantial reduction demonstrates that the segmented boundaries produced by Adaptive Erosion more closely align with the ground truth, preserving the true shape of waterbodies more effectively. Furthermore, the Boundary F1 Score, a crucial metric for assessing the accuracy of edge detection, improved from 0.0519 ± 0.0170 (SLIC) to 0.0695 ± 0.0207 (Adaptive Erosion), reflecting a 33.9% increase. This higher F1 score indicates a notable enhancement in boundary alignment, with fewer false positives and false negatives, leading to more precise and reliable segmentation results.

Table 4: Statistical Comparison of Segmentation Metrics Between SLIC Original and Adaptive Erosion

Metric	SLIC Original (Mean ± Std Dev)	Adaptive Erosion (Mean ± Std Dev)	Percentage Change
OSR	0.7550 ± 0.1494	0.7574 ± 0.1462	+0.32% (slightly increased)
Hausdorff Distance	325.8278 ± 131.4516	216.3736 ± 94.0054	-33.6% (significantly reduced)
Boundary F1 Score	0.0519 ± 0.0170	0.0695 ± 0.0207	+33.9% (significant improvement)

Based on the evaluation metrics, a key conclusion is that the adaptive erosion method significantly enhances boundary extraction, a critical aspect of accurate segmentation. The substantial reduction in Hausdorff Distance (-33.6%) and the dramatic increase in the Boundary F1 Score (+33.9%) provide strong evidence that our method is highly effective at precisely delineating the boundaries of waterbodies. While the Overall Segmentation Result (OSR) showed only a marginal improvement (+0.32%), this reinforces the fact that the method's primary benefit lies in its ability to refine the edges, a crucial capability for applications like flood mapping where the exact perimeter is essential for accurate measurement.

Optimization of Structuring Element Size

To identify the optimal kernel size and number of iterations for morphological processing in the

Adaptive Erosion method, a set of experiments was conducted. The Dice Similarity Coefficient (DSC) was used as the primary evaluation metric to quantify segmentation accuracy for each configuration. Table 5 evaluate the Dice Similarity Coefficient (DSC) for Different Kernel Sizes. The 3×3 kernel consistently achieved the highest average DSC of 0.87037, indicating that smaller kernel sizes preserve more detail and provide superior segmentation accuracy for the given dataset. The data strongly suggests that the 3x3 structuring element is the optimal kernel size for this segmentation task. Using larger kernels leads to over-erosion, which negatively impacts the overall segmentation accuracy as measured by the DSC. This finding justifies the use of smaller, fine-tuned kernels for adaptive erosion in the proposed method.

Table 5: Evaluation of Dice Similarity Coefficient (DSC) for Different Kernel Sizes

Image Sample	3×3	5×5	7×7
1.jpg	0.95654	0.93869	0.91023
2.jpg	0.95503	0.93425	0.88208
3.jpg	0.91940	0.89878	0.88887
4.jpg	0.77255	0.67336	0.56395
5.jpg	0.88178	0.80470	0.74977
6.jpg	0.92011	0.85557	0.76670
7.jpg	0.71718	0.78056	0.78584
8.jpg	0.86503	0.81432	0.75300
9.jpg	0.87019	0.86949	0.85172
10.jpg	0.84588	0.78933	0.78538
Average	**0.87037**	**0.83591**	**0.79375**

Table 6 presents the adaptive selection of erosion kernel size based on the computed local intensity variance of each input image. The variance serves as a quantitative indicator of brightness variation, noise level, and texture complexity. Images with lower variance values require moderate erosion and are processed using a 5×5 kernel, whereas images exhibiting higher variance are assigned a larger 7×7 kernel to effectively suppress noise and reduce over-segmentation. This table demonstrates that kernel selection in the proposed method is guided by image statistics rather than heuristic or manual tuning, ensuring adaptive and reproducible segmentation behavior.

Table 7 demonstrates that increasing the number of iterations improves segmentation accuracy up to a point. The highest DSC value 0.8617 was observed at 6 iterations, while 9 iterations resulted in a slight decline. Therefore, 6 iterations are identified as the optimal choice to balance accuracy and computational efficiency.

Table 6: Adaptive Kernel Selection Based on Local Intensity Variance

Image Sample	Local Variance	Selected Kernel
1.jpg	0.019514	5x5
2.jpg	0.057561	7x7
3.jpg	0.074995	7x7
4.jpg	0.064638	7x7
5.jpg	0.036005	7x7
6.jpg	0.036147	7x7
7.jpg	0.060635	7x7
8.jpg	0.059984	7x7
9.jpg	0.026758	7x7
10.jpg	0.029636	7x7

Table 7: Effect of Iteration Count on Dice Similarity Coefficient (DSC)

Iteration Count	DSC Score
3 Iterations	0.6756
6 Iterations	0.8617
9 Iterations	0.8473

Qualitative Analysis of Superpixel with Colorization Technique

For the evaluation of the proposed method, ten random images with a water area are subjected to segmentation. This superpixel based method works by assigning unique colors to pixels in the image to make analysis easier. Certain ranges of colors red, green and blue are chosen by hand, and pixels that meet specific criteria based on the average colors of pixels in their area are changed to white to make them easier to spot. This approach helps show how strong the colors are in different parts of an image and makes all the pixel values in the image the same, which is especially useful for water area detection.

Random images from Figure 6, labelled (A) to (E), were selected for image segmentation. The second column displays the corresponding ground truth images for comparing the segmentation results. The third column shows superpixels created for the segmentation process. The fourth column presents the final results of the segmentation technique applied to the images. Superpixel shows the K-means clustering of pixels. In the proposed method predefined pixel values are considered for water area detection. Pixels that satisfy conditions are transformed into white pixels. It provides uniqueness in pixel orientation thus, superpixel generation will be improving. Visual representations of segmentation without the erosion technique is shown in Figure 6.

Qualitative Analysis of Enhanced Segmentation with Adaptive Erosion Technique

Visual representation of enhanced image segmentation using erosion technique is shown in Figure 7. Here input images are show in first column (A) to (E) are applied for enhanced segmentation algorithm. Second column shows ground truth image, next column represents the eroded image after applying erosion technique. These images have water areas are more lighter and region other than water gets darker. Thus, the accuracy of superpixel generation will be improving. Fourth column shows generated superpixels, compared with third column of Figure 6 more number of accurate superpixels are generated. Fifth column shows the segmentation mask.

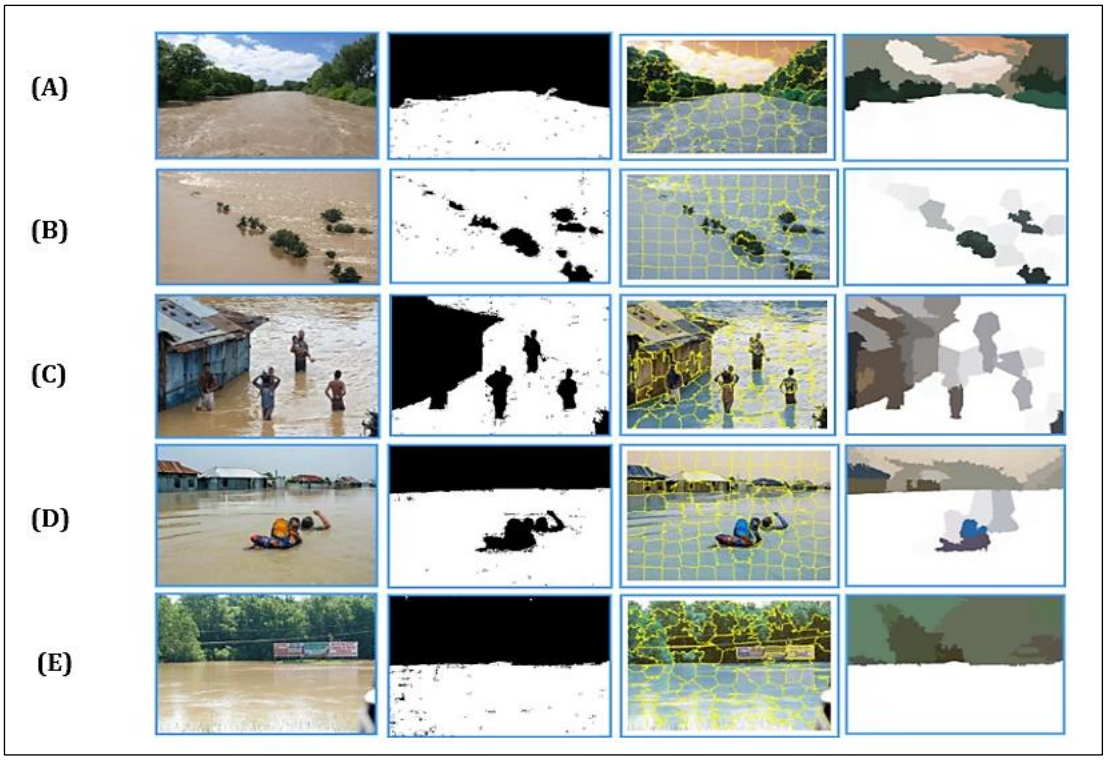

Figure 6: (First Column) Test Images (A–E) (Second Column) Ground Truth Images (Third Column) Generated Superpixels, (Fourth Column) Segmented Output

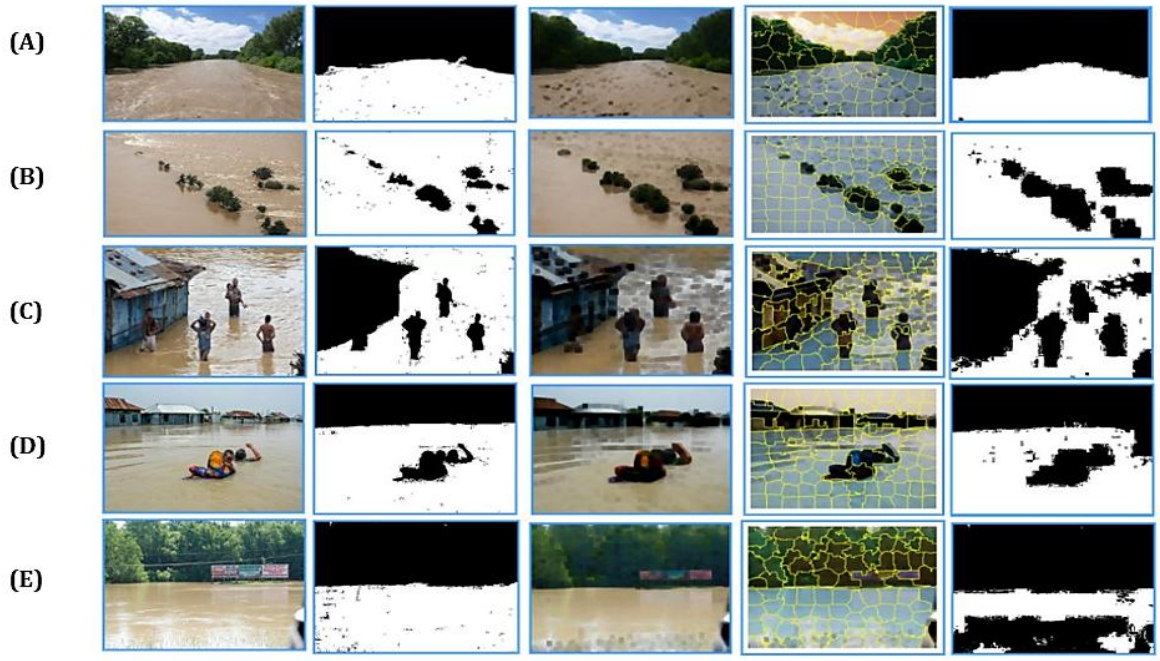

Figure 7: (First Column) Test Images (A–E) (Second column) Ground Truth Images (Third column) Generated Superpixel (Fourth column) Segmented Output (Fifth Column) Segmentation Mask

Improvement in Dice Similarity using Adaptive Erosion-Based Segmentation

The effectiveness of the proposed method was assessed using the Dice Similarity Coefficient (DSC), which quantifies the similarity between two sets. DSC compares the shared elements to the total elements in both sets and is commonly used to evaluate image segmentation accuracy. Table 8 presents a comparison before and after applying an erosion technique. Six images exhibited significant improvement in DSC values, indicating enhanced segmentation accuracy. Although

certain images showed a slight decline in segmentation accuracy due to complex pixel structures and varying object boundaries, the overall performance of the pro- posed adaptive erosion-based segmentation technique remained superior. As illustrated in Table 9, the integration of adaptive erosion significantly improved the segmentation results. The analysis was carried out on multiple test images from specific domains, and the average performance of the processed images was evaluated. Table 10 provides a comparative analysis of the Dice Similarity Coefficient values between the traditional superpixel based segmentation and the enhanced adaptive erosion-based segmentation approach, demonstrating the effectiveness and improved accuracy of the proposed method.

Table 8: Quantitative Effectiveness of the Proposed Algorithm

Image Sample	DSC Value of Normal Superpixel	DSC Value of Enhanced Superpixels
1.jpg	0.74	0.95
2.jpg	0.85	0.96
3.jpg	0.91	0.88
4.jpg	0.64	0.81
5.jpg	0.93	0.91
6.jpg	0.94	0.91
7.jpg	0.87	0.64
8.jpg	0.66	0.86
9.jpg	0.87	0.89
10.jpg	0.86	0.93

Table 9: Quantitative Metrics

Metric	Before Erosion	After Erosion
OSR	0.21	0.13
Boundary F1-Score	0.76	0.84
Hausdorff Distance	12.8	8.3
EPE	4.2	2.6

Table 10: Quantitative Metrics

Image Segmentation Method	Average DSC Value
Superpixel based Segmentation	0.82
Enhanced Superpixel based Segmentation with Erosion Technique	0.87

Benchmarking Against Conventional SLIC-Based Segmentation

To comprehensively evaluate the proposed Adaptive Erosion-based superpixel segmentation method, a comparative study was conducted against the conventional SLIC-based segmentation approach. The evaluation focused on five key performance metrics: Jaccard Index, Precision, Recall, Boundary F1 Score, and Runtime. These metrics are essential for understanding both the accuracy and efficiency of a segmentation method. The results are summarized in Table 11 below.

Figure 8 compares the performance of the SLIC-based method and the proposed adaptive erosion-based segmentation across key metrics. The Adaptive Erosion model outperforms SLIC in Jaccard Index, Recall, Boundary F1 Score, Runtime, and DSC, demonstrating better accuracy and efficiency. While SLIC shows slightly higher precision, Adaptive Erosion offers more balanced and robust segmentation, making it suitable for real-time and remote sensing applications. The results indicate that the proposed model outperforms the baseline in most of the evaluated metrics. The Jaccard Index for Adaptive Erosion is higher than that of SLIC, indicating a more accurate overlap between the segmented output and ground truth. This improvement demonstrates the enhanced region-wise accuracy achieved by the proposed method. In terms of recall, the Adaptive Erosion model also performs better, capturing a larger proportion of relevant regions (e.g., water bodies). This is particularly beneficial in remote sensing applications where missing true positives can result in significant errors in analysis or decision-making.

Table 11: Comparative Performance Metrics between SLIC and Adaptive Erosion-Based Segmentation

Metric	SLIC	Adaptive Erosion	Better Model / Improvement
Jaccard Index	0.7653	0.7751	Adaptive Erosion (+1.3%)
Precision	0.9985	0.9776	SLIC (Higher Precision)
Recall	0.7664	0.7916	Adaptive Erosion (+3.3%)
Boundary F1 Score	0.0347	0.0598	Adaptive Erosion (+72.3%)
Runtime (s)	0.8090	0.4143	Adaptive Erosion (2× Faster)

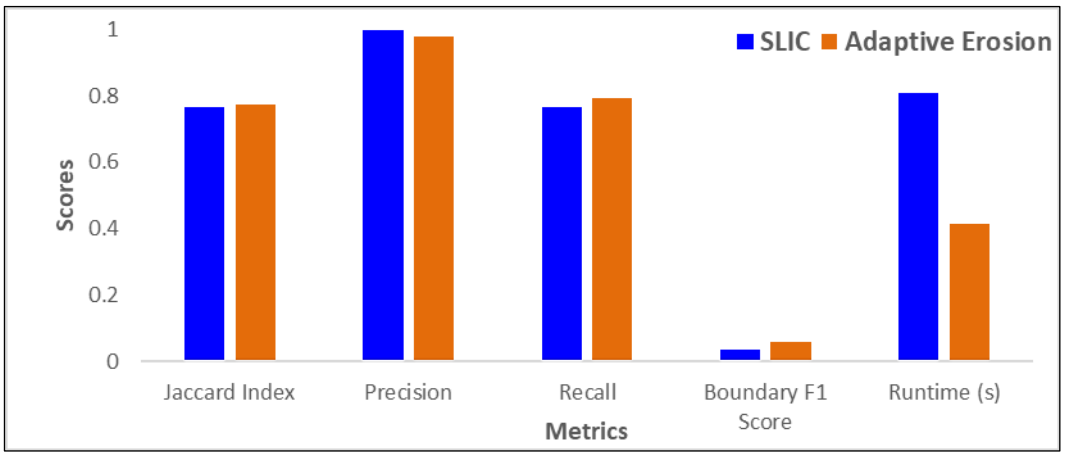

Figure 8: Performance Comparison of SLIC and Adaptive Erosion-Based Segmentation

Although the SLIC model yields slightly higher precision, this can be attributed to its conservative nature, which may result in a higher number of false negatives. In contrast, Adaptive Erosion achieves a more balanced trade-off between precision and recall, which is reflected in its improved Jaccard Index and overall segmentation quality. One of the most notable improvements is observed in the Boundary F1 Score, where the Adaptive Erosion model shows a 72.3% increase over SLIC. This indicates superior boundary preservation, making the method highly suitable for applications requiring accurate delineation of object edges, such as shoreline extraction or flood boundary mapping. Additionally, the proposed method demonstrates superior computational efficiency, reducing the run- time by nearly half compared to SLIC. This efficiency makes it more practical for large-scale image analysis or real-time processing scenarios.

Overall, the Adaptive Erosion-based segmentation method outperforms SLIC by providing better results in terms of Jaccard Index, recall, boundary accuracy, and runtime efficiency for superpixel-based image segmentation in remote sensing applications.

Statistical Validation of Performance Improvement

This section analyses the improvements in the proposed adaptive erosion-based method by the random fluctuations or not. For the evaluation of this method paired sample t-test was performed on the Dice Similarity Coefficient values. It is more suitable to compare two sets of values to find out if they are significantly different from each other. Normal and proposed image segmentations are evaluated using the same segmentation method namely Dice Similarity Coefficient, these two-method subjected for same set of images. So, t- test provide a good model validation. The test was performed using DSC scores obtained from 10 randomly selected flood-affected images. Since each image was segmented using both methods, the paired t-test was appropriate to determine whether the differences in performance were statistically significant. Table 12 revealed a p-value of 0.0174 and an average improvement of 0.05 in DSC. If the p-value is less than 0.05, the difference is statistically significant, indicating that the improvement is not the result of chance. The upgraded technique consistently outperforms the baseline, as evidenced by the 95% confidence interval for the mean difference, which was 0.011, 0.089. For flood prediction tasks, the suggested

adaptive erosion-based segmentation strategy provides a notable and reliable improvement over conventional methods for waterbody detection, as supported by this statistical validation.

The comprehensive statistical analysis presented here provides strong evidence that the proposed adaptive erosion-based method represents a significant and reliable advancement for waterbody detection in flood prediction. The paired sample t-test's (df = 9) p-value of 0.0174, being well below the 0.05 threshold, confirms that the observed average improvement of 0.05 in the Dice Similarity Coefficient is not due to random chance but is a statistically significant enhancement. Furthermore, the obtained Cohen's *d* value of 0.78 indicates a moderate-to-large effect size, demonstrating that the performance gain of the proposed method is not only statistically significant but also practically meaningful. This quantitative validation, combined with the qualitative visual evidence, demonstrates that the upgraded technique consistently and accurately outperforms conventional segmentation methods, making it a robust and trustworthy tool for a wide range of flood prediction applications.

Table 12: Statistical Comparison of DSC Values Between Normal and Enhanced Segmentation

Metric	Superpixel Segmentation	Adaptive Erosion Segmentation	Mean Difference	df	p-value	Cohen's d	95% Confidence Interval
Dice Similarity Coefficient	0.82 (average)	0.87 (average)	+0.05	9	0.0174	0.78	(0.011, 0.089)

Comparative Analysis with State-of-the-Art Methods

Table 13 presents a comparative analysis of the proposed segmentation method against several established algorithms, including GS04 (25), NC05 (26), GCb10^b (27), TP09^b (28), QS09 (2), and the widely-used SLIC (18). The comparison is based on three key metrics: under-segmentation error, boundary recall, and segmentation accuracy. Under-segmentation Error reflects the degree to which image segments incorrectly merge with adjacent regions. A lower value indicates more precise boundary adherence. The proposed method achieves the lowest under-segmentation error of 0.18, outperforming GS04 (25) (0.23), NC05 (26) and GCb10^b (26) (0.22 each), TP09^b (27) (0.24), QS09 (28) (0.20), and even SLIC (18) (0.19). This result highlights the effectiveness of the proposed approach in preserving region integrity and reducing leakage across boundaries. Boundary Recall measures how well the segmentation captures actual object boundaries. While GS04 (25) and SLIC (25) attain the highest recall scores of 0.84 and 0.82 respectively, the proposed method also performs strongly with a boundary recall of 0.79—surpassing NC05 (23, 24) (0.68), GCb10^b (28) (0.70), and TP09^b (27) (0.61). This indicates the proposed method's strong edge-preservation capabilities.

Segmentation Accuracy, which represents the percentage of correctly classified segments relative to ground truth, is where the proposed method excels. It achieves an accuracy of 87%, significantly outperforming SLIC (25) (76.9%), NC05 (26) (75.9%), QS09 (28) (75.1%), and other classical methods such as GS04 (28) (74.6%), GCb10^b (28) (73.2%), and TP09^b (28) (62.0%).

In summary, the proposed segmentation framework demonstrates a balanced and superior performance across all three evaluation criteria. By minimizing under-segmentation error, maintaining high boundary recall, and achieving the highest segmentation accuracy, it proves to be a robust solution for flood-related waterbody detection in satellite imagery.

Table 13: Comparison with Existing Methods

Metric	GS04 (25)	NC05 (26)	GCb10^b (26)	TP09^b (27)	QS09 (27)	SLIC (18)	Proposed Method
Under-segmentation error	0.23	0.22	0.22	0.24	0.20	0.19	0.18
Boundary recall	0.84	0.68	0.70	0.61	0.79	0.82	0.79
Segmentation accuracy	74.6%	75.9%	73.2%	62.0%	75.1%	76.9%	87%

Conclusion

In this study, an adaptive erosion-based superpixel segmentation approach was proposed for accurate waterbody detection in flood prediction applications. The integration of adaptive erosion with SLIC-based superpixel segmentation effectively addressed the challenges of misclassification and over-segmentation, particularly in complex environments where water regions exhibit similar visual characteristics to surrounding objects such as rooftops, land, and varying water textures. The adaptive erosion technique contributed significantly to boundary refinement and noise reduction, enhancing the clarity and accuracy of segmented regions.

The experimental evaluation demonstrated the superiority of the proposed method over conventional SLIC segmentation, achieving notable improvements in key performance metrics. Specifically, the method attained a 1.3% increase in Jaccard Index, a 3.3% enhancement in Recall, a substantial 72.3% improvement in Boundary F1 Score, and a twofold reduction in computational runtime. These results highlight the robustness, accuracy, and computational efficiency of the proposed technique, establishing its potential for real-time flood monitoring, waterbody detection, and other remote sensing applications in disaster management.

Abbreviations

ANN: Artificial Neural Network, BA-DEA: Buttle-net Attacking based Dolphin Echolocation Algorithm, DSC: Dice Similarity Coefficient, FN: False Negative, FP: False Positive, IoU: Intersection over Union, OSR: Over-Segmentation Rate, RGB: Red, Green, Blue, SLIC: Simple Linear Iterative Clustering, TP: True Positive.

Acknowledgement

None.

Author Contributions

Jyothish VR: conceptualization, methodology design, data collection, analysis, visualization, preparation of the initial manuscript draft, Sajimon Abraham: supervision, overall research guidance, Leo Abraham: validation, manuscript editing, Sabu Augustine: data analysis, interpretation of results.

Conflict of Interest

The authors declare no conflict of interest, financial or otherwise.

Declaration of Artificial Intelligence (AI) Assistance

The authors declare no use of artificial intelligence (AI) for the write-up of the manuscript.

Ethics Approval

Cross-sectional survey-based research, such as the present one, is typically exempted from the Institute Review Board approval under 45 CFR 46.101(b): Categories of Exempt Human Subjects Research. No animals were involved in the research. The ethical guidelines involving human subjects provided by the American Psychological Association were strictly followed.

Funding

None.

References

1. Muhadi NA, Abdullah AF, Bejo SK, Mahadi MR, Mijic A. Image segmentation methods for flood monitoring system. Water. 2020; 12(6):1825. https://doi.org/10.3390/w12061825
2. Hernández D, Cecilia JM, Cano JC, Calafate CT. Flood detection using real-time image segmentation from unmanned aerial vehicles on edge-computing platform. Remote Sensing. 2022;14(1):223. https://doi.org/10.3390/rs14010223
3. Huang S, Jin X, Jiang Q, Liu L. Deep learning for image colorization: Current and future prospects. Engineering Applications of Artificial Intelligence. 2022;114: 105006. https://doi.org/10.1016/j.engappai.2022.105006
4. Xu Q, Wu L, Zhang W, *et al*. Mapping water bodies under cloud cover using remotely sensed optical images and a spatiotemporal dependence model. Int J Appl Earth Obs Geoinf. 2021;103: 102470. https://doi.org/10.1016/j.jag.2021.102470
5. Stateczny A, Praveena HD, Krishnappa RH, *et al*. Optimized deep learning model for flood detection using satellite images. Remote Sensing. 2023; 15(20):5037. https://doi.org/10.3390/rs15205037
6. Troya-Galvis A, Gançarski P, Passat N, Berti-Equille L. Unsupervised quantification of under- and over-segmentation for object-based remote sensing image analysis. IEEE J Sel Top Appl Earth Obs Remote Sens. 2015; 8(5):1932–1945.
7. Sivakumar P, Meenakshi S. A review on image segmentation techniques. Int J Adv Res Comput Eng Technol. 2016; 5(3):1045–1050.
8. Wang M, Dong Z, Cheng Y, Li D. Optimal segmentation of high-resolution remote sensing image by combining superpixels with the minimum spanning tree. IEEE Trans Geosci Remote Sens. 2018; 56(5):2998–3011.

9. Said KAM, Jambek AB. Analysis of image processing using morphological erosion and dilation. J Phys Conf Ser. 2021; 2071:012033. https://doi.org/10.1088/1742-6596/2071/1/012033
10. Pal NR, Pal SK. A review on image segmentation techniques. Pattern Recognit. 1993;26(9):1277–1294. https://doi.org/10.1016/0031-3203(93)90135-J
11. Chen S, Huang W, Chen Y, Feng M. An adaptive thresholding approach toward rapid flood coverage extraction from Sentinel-1 SAR imagery. Remote Sensing. 2021; 13(23):4899.
12. Tu B, Kuang W, Zhao G, Fei H. Hyperspectral image classification via superpixel spectral metrics representation. IEEE Signal Process Lett. 2018; 25(5):636–640.
13. Achanta R, Shaji A, Smith K, Lucchi A, Fua P, Süsstrunk S. SLIC superpixels compared to state-of-the-art superpixel methods. IEEE Trans Pattern Anal Mach Intell. 2012; 34(11):2274–2282. https://doi.org/10.1109/TPAMI.2012.120
14. Miyamoto T. Superpixel classification with the aid of neighborhood for water mapping in SAR imagery. Remote Sensing. 2024; 16(23):4576. https://doi.org/10.3390/rs16234576
15. Levin A, Lischinski D, Weiss Y. Colorization using optimization. ACM Trans Graph. 2004; 23(3):689–694. https://doi.org/10.1145/1015706.1015780
16. Li B, Zhao F, Su Z, Liang X, Lai YK, Rosin PL. Example-based image colorization using locality-consistent sparse representation. IEEE Trans Image Process. 2014; 23(11):4899–4912.
17. Tiwari V, Kumar V, Matin MA, *et al*. Flood inundation mapping—Kerala 2018: Harnessing the power of SAR, automatic threshold detection method and Google Earth Engine. PLoS One. 2020; 15(8): e0237324. https://doi.org/10.1371/journal.pone.0237324
18. Ghoish B, Garg S, Motagh M, Martinis S. Automatic flood detection from Sentinel-1 data using a nested UNet model and a NASA benchmark dataset. PFG – J Photogramm Remote Sens Geoinf Sci. 2024; 92:1–12. https://doi.org/10.1007/s41064-024-00275-1
19. Mehra J, Neeru N. A brief review: Super-pixel based image segmentation methods. Imperial J Interdiscip Res. 2016; 2(5):2454–1362.
20. Felzenszwalb PF, Huttenlocher DP. Efficient graph-based image segmentation. Int J Comput Vis. 2004; 59(2):167–181. https://doi.org/10.1023/B:VISI.0000022288.19776.77
21. Shi J, Malik J. Normalized cuts and image segmentation. IEEE Trans Pattern Anal Mach Intell. 2000;22(8):888–905. https://doi.org/10.1109/34.868688
22. Fan Y-R. Robust superpixel segmentation for hyperspectral-image restoration. Entropy. 2023; 25(2):260. https://doi.org/10.3390/e25020260
23. Jyothish VR, Bindu MS, Greeshma MS. An efficient image segmentation approach using superpixels with colorization. Procedia Comput Sci. 2020;171: 837–846.
24. Vedaldi A, Soatto S. Quick shift and kernel methods for mode seeking. Proceedings of the European Conference on Computer Vision (ECCV). 2008; 5305: 705–718. doi: 10.1007/978-3-540-88693-8_52
25. Veksler O, Boykov Y, Mehrani P. Superpixels and supervoxels in an energy optimization framework. Proceedings of the European Conference on Computer Vision (ECCV). 2010; 6315: 211–224. https://doi.org/10.1007/978-3-642-15555-0_16
26. Levinshtein A, Stere A, Kutulakos KN, Fleet DJ, Dickinson SJ, Siddiqi K. Turbopixels: Fast superpixels using geometric flows. IEEE Trans Pattern Anal Mach Intell. 2009; 31(12):2290–2297. https://doi.org/10.1109/TPAMI.2009.96
27. Li C, Anwar S, Tahir M, Mian A, Khan F, Muzaffar A. Image colorization: A survey and dataset. IEEE Access. 2020; 8:123234–123249. https://doi.org/10.48550/arXiv.2008.10774
28. Zhu A, Mei J, Qiao S, Yan H, Zhu Y, Chen LC, Kretzschmar H. Superpixel transformers for semantic segmentation. IEEE Trans Pattern Anal Mach Intell. 2023; 45(3):2345–2357.

How to Cite: Jyothish VR, Abraham S, Abraham L, Augustine S. Superpixel-Based Image Segmentation with Adaptive Erosion for Waterbody Detection in Flood Prediction. Int Res J Multidiscip Scope. 7(1):1389-1407. DOI: 10.47857/irjms.2026.v07i01.08027